Thermal behaviour of masonry walls: Mathematical modelling and field monitoring

Chidiac, S. E.; Maurenbrecher, A. H. P.; Guan, W.

Publisher's version / Version de l'éditeur:
https://doi.org/10.1080/09613219308727317
Building Research and Information, 21, 5, pp. 280-287, 1993-09

Thermal behaviour of masonry walls: Mathematical modelling and field monitoring

NRCC-36097

Chidiac, S.E.; Maurenbrecher, A.H.P.; Guan, W.

September 1993

A version of this document is published in / Une version de ce document se trouve dans: *Building Research and Information,* 21, (5), pp. 280-287, September 1993, DOI: 10.1080/09613219308727317

Thermal behaviour of masonry walls: mathematical modelling and field monitoring

FINITE ELEMENT DISCRETIZATION PROCEDURE USED TO SOLVE HEAT BALANCE EQUATION – RESULTS ARE IN GOOD AGREEMENT WITH FIELD DATA

S. E. Chidiac, A. H. P. Maurenbrecher and W. Guan

Structures Laboratory. The Institute for Research and Construction, The National Research Council, Ottawa, Ontario, K1A 0R6 Canada

This Canadian study shows that the potential use of their procedure is very broad since the data computed can be used to investigate deterioration problems, to check risks associated with any proposed thermal upgrading and to perform stress analysis. The variation between the computed data and recorded data is small, except at peaks where the maximum differences occur.

Cette étude canadienne montre que l'utilisation potentielle de leur procédure est très étendue puisqu'on peut se servir des données traitées pour examiner les problèmes de degradation, contrôler les risques associées à toute amélioration thermique proposée et effectuer des analyses de contraintes. Il y a très peu de différence entre les données traitées par informatique et les valeurs relevées sur place, sauf au moment des pointes lorsque la différence est au maximum.

Keywords: masonry walls, thermal behaviour, mathematical modelling, Canada

Mathematical modelling in association with field monitoring is proposed to study the thermal behaviour of masonry walls. The mathematical model solves the heat balance equation using the finite element discretization procedure. Monitoring is performed to collect data to be used as boundary conditions for the dynamic analysis and to check the results. The feasibility of such a procedure is demonstrated by a case study involving a masonry building. Results obtained from the mathematical model are in good agreement with the field data where the average error is found to be 4.3% after the first 1000h. The variations in the results due to the initial temperature, thermophysical properties and boundary conditions are discussed in this paper.

Introduction

Replacement of existing buildings with new ones has become less acceptable given the current economic conditions, not to mention the environmental impact of demolition waste. Thus the subjects of upgrading and investigation of deterioration are of increasing interest to both owners and engineers. To address the topic of rehabilitation, engineers must survey the structure and in some cases may want to monitor its behaviour. There are numerous reasons for thermal monitoring of masonry walls:

- to gain insight into causes of deterioration,
- to explore any side effects of thermal upgrading,
- to determine frost penetration,
- to check the thermal resistance of the wall

But monitoring alone can be expensive, time consuming, and inconclusive. Mathematical modelling in association with monitoring will reduce the number of sensors needed and at the same time give a better understanding of the behaviour of the masonry wall.

The objectives of this paper are two-fold: first, to show how a mathematical method can be used to investigate the temperature in masonry walls in conjunction with minimal field data, and second, to discuss the possible factors affecting the reliability of this approach.

In this paper, the heat balance equation for the model is first briefly presented and its solution by the finite element is described. Field monitoring and a method of implementation are discussed next. The potential of the proposed approach is then explored by comparing computed results to temperature data collected in the field.

Heat balance equations and boundary conditions

Multi-dimensional transient heat conduction is governed by the following differential equation:

$$\rho \frac{\partial H}{\partial \tau} = \Delta \cdot (k \nabla T) + \Phi \tag{1}$$

where ρ, H, k, Φ, T and τ are density, enthalpy, conductivity, rate of heat generation per unit volume, temperature, and time, respectively. The enthalpy is defined as the sum of the sensible and latent heat; the latter needs to be included whenever a phase change occurs.

Since we are dealing with a boundary-value problem, the heat flow is controlled by the boundary conditions, namely:

- Dirichlet boundary condition, where the temperature is specified for a given surface of the body, or
- Cauchy boundary condition, where all modes of heat transfer occur, namely conduction, convection, and radiation.

The transient heat flow equation is solved on the basis of the finite element method [1], where the isoparametric finite-element is used for spacewise discretization and the two-point recurrence scheme for temporal discretization. The discretized equations for the heat balance are obtained using the method of weighted residuals along with the Galerkin weighting procedure [2].

In order to perform the analysis, both the thermophysical properties and the boundary conditions have to be defined. In this study, the thermophysical properties were not measured, rather properties listed in the literature were used [3, 4, 6]. The boundary conditions are difficult to quantify given the dynamic nature of the outside environment. To overcome this difficulty, field data are inserted into the model instead.

Field monitoring

Long term monitoring is used to help understand the behaviour of buildings and to check design assumptions and theoretical predictions. Monitoring of actual performance while a building is in service can also be used to detect faults and deterioration at an early stage.

Mathematical modelling in conjunction with monitoring leads to a reduced number of sensors and increases the degree of certainty in the mathematical analysis. This combination will significantly reduce costs, since the installation and calibration of sensors is time consuming and often requires special equipment such as swing stages or hydraulic hoists. Moreover, installing fewer sensors outside and inside a building reduces the inconvenience for the occupants.

Method of implementation

The proposed method of investigation is composed of two steps:

Monitoring

Only one outside temperature sensor per floor is needed for an exterior wall of interest, preferably at the mid-height of every storey. The inside surface temperature also must be monitored, but no sensors are needed within the wall, ie opening up or drilling is not required. For investigations into specific problems such as thermal bridging, sensors may be needed in these locations to generate input data for the mathematical model. The duration of the monitoring may be limited by tight schedule; however, to obtain a good picture of the dynamic thermal behaviour of the masonry wall, monitoring of at least 18 months is recommended especially if there is moisture movement within the wall.

Mathematical model

A numerical model can be generated to represent the composition and geometry of the wall to be monitored. Although the finite element method is used in this study, other methods such as finite difference, finite volume, should yield similar results. The measured exterior and interior surface temperatures can be inserted into the model using the Dirichlet boundary condition.

Once these two steps are completed, the time-history of the temperature field can be obtained everywhere in the wall system. The feasibility of this approach will now be assessed through a case study.

Case study

Maurenbrecher and Suter [5, 6] have investigated the exterior clay brick walls in a five-storey loadbearing masonry building. Both temperature and moisture were monitored in an area which had suffered frost damage. The condition of the building and the monitoring procedure have been reported in the references but for clarity a brief description is also given in this paper.

The geometry of the walls monitored and the wall composition are shown in Figs 1 and 2, respectively. Seventeen temperature sensors were used and their locations were marked on Fig. 1. Because of disruptions while recording, only four months of continuous data are available starting 1 April 1988. The data were logged every hour.

The finite element mesh for the three-dimensional heat flow analysis along with the dimensions of the wall and the boundary conditions are shown in Fig. 3. The NE wall is divided into 19 finite-elements along the length, 12 along the height and 6 along the depth whereas the SE wall has 19, 12 and 7 finite-elements along the length, height and depth, respectively. The total number of 3-D eight-node isoparametric elements used in the analysis is 2364

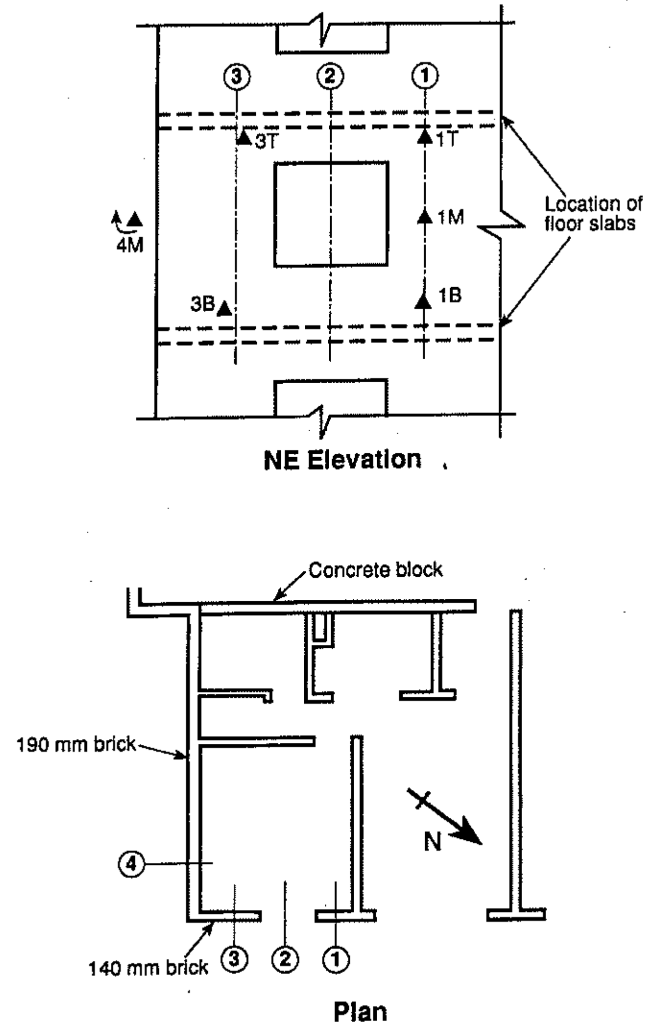

Fig. 1. View of the wall analysed showing locations of temperature sensors.

having 3109 nodes. The time step used in the analysis is one hour. Both temporal and spatial discretization are critical to the accuracy of the analysis. The criterion for size of element [7]

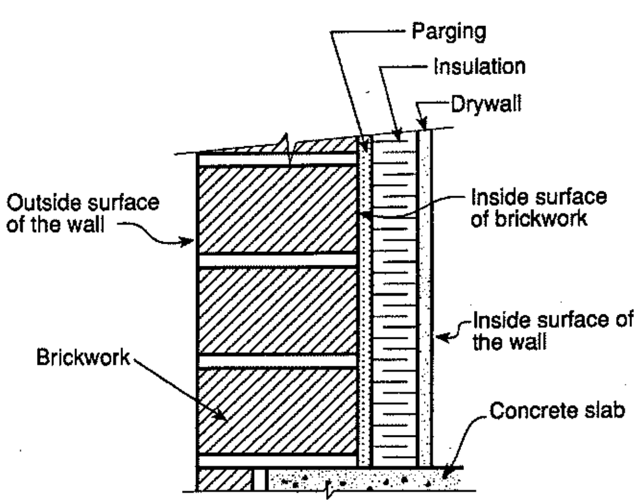

Fig. 2. Cross-section view of the masonry wall.

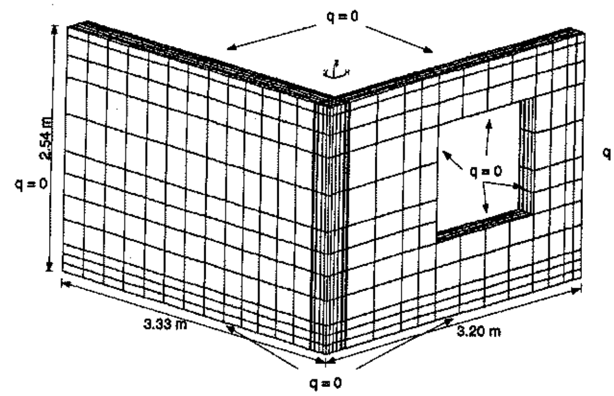

Fig. 3. Model analysis of the masonry wall.

to reduce numerical oscillations for this type of investigation is:

$$\frac{\Delta x^2}{\alpha\, \Delta \tau} = 2.26 \qquad (2)$$

in which α, Δx and $\Delta \tau$ are the diffusivity, element size and time step, respectively. To include the effect of thermal bridging, part of the concrete slab has been included in the analysis. The effects of the window were ignored.

In the analysis, the temperature for the outside face of the wall is set to be the same as the field data. One sensor is used for the NE wall and one for the SE wall. The outside surface temperature of the masonry wall and not the outside air temperature is recommended for this kind of investigation because of difficulties that are encountered when incorporating the effects of solar radiation, wetness and wind speed. This can be seen in Fig. 4 where the SE wall is more exposed to solar radiation and as much as 10–15 °C differences occur between peaks of outside air temperature and the wall surface temperature. To allow for all of these effects in a numerical model is extremely difficult, which has led to the present approach of combining mathematical modelling with monitoring. The data employed in the analysis are shown in Figs 5 and 6.

The same procedure is used for the inside surface of the wall to reduce uncertainty in defining the convective surface heat coefficient. The temperature on the inside face of the wall is assumed uniform for both the NE and SE wall and the values used are shown in Fig. 7.

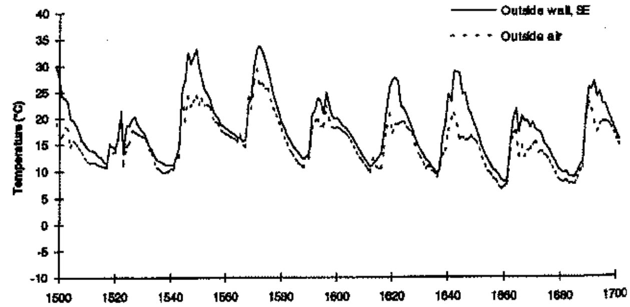

Fig. 4. Measured outside air and outside surface temperature of SE wall for a period of 200 h.

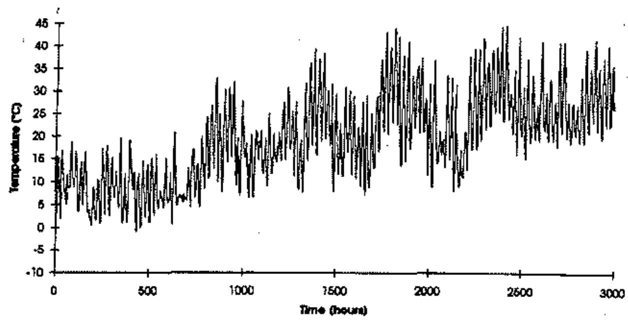

Fig. 5. Measured outside surface temperature of NE wall used as input to the FE analysis (location 1M).

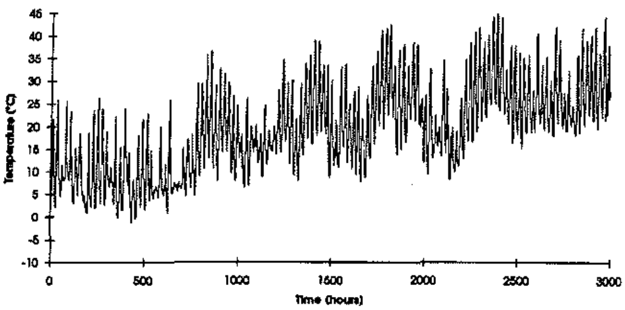

Fig. 6. Measured outside surface temperature of SE wall used as input to the FE analysis (location 4M).

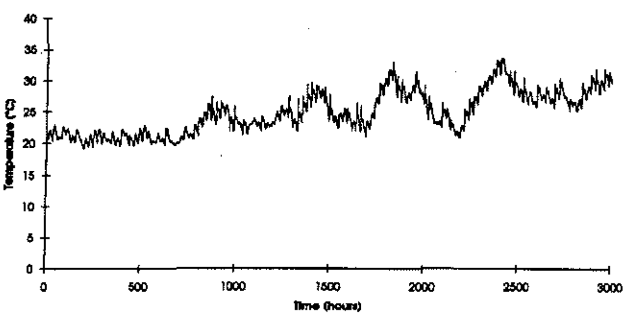

Fig. 7. Measured inside surface temperature of walls used as input to the FE analysis (location 1M).

The initial temperature of the wall used in the model is assumed constant and equal to 0° C. The value of zero is used in this study first, to check how long it takes the model to equilibrate itself and second, to examine whether any numerical oscillation will occur. Two sets of thermophysical properties [3, 4, 6] are employed in the finite element analysis and the values are listed in Table 1. This is done in order to give an indication of how the properties affect the overall temperature distribution since the value for the properties used are an approximation. The computations were carried out with a SUN SPARC 10 workstation, a 1.0 Gigabyte hard disk and the finite element program AFEMS [8]. The computational time required to perform a 3000h simulation is 3.8 days. A large amount of data was obtained from the dynamic analysis; only a summary is presented here.

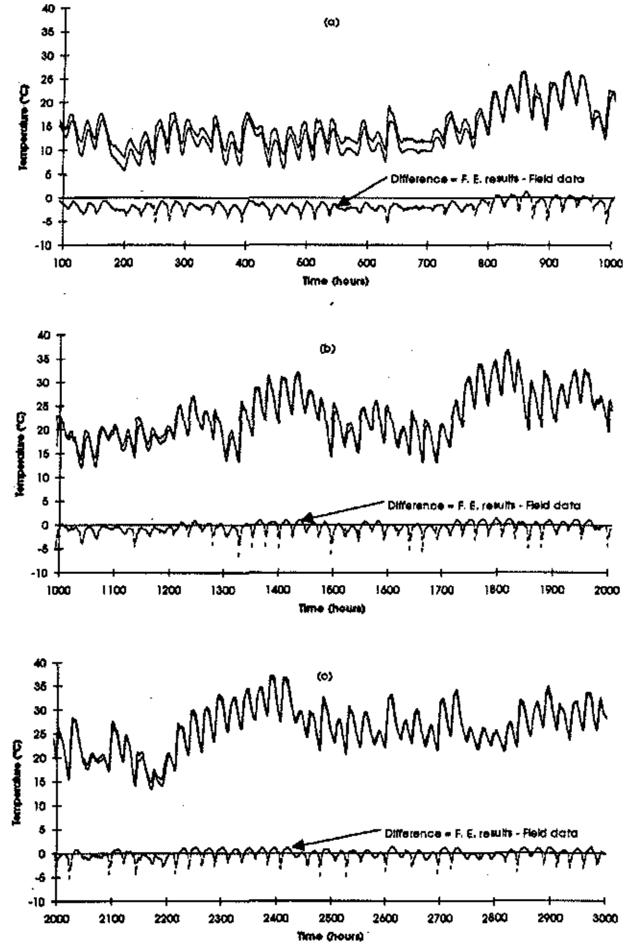

Fig. 8. FE results, field data and the difference between the two values for location 1T; (a) 100–1000 h, (b) 1000–2000 h, (c) 2000–3000 h.

The temperature on the inside face of the brick wall is used as the check value for the results

Table 1. Thermophysical properties used in the FE analysis

Material	Thermal conductivity ($W m^{-1}$ °K)		Density (kg per m^3)		Specific heat ($J kg^{-1}$ °K)	
	First run	Second run	First run	Second run	First run	Second run
Brick	0.72	0.80	1950	2000	840	840
Parging	0.72	0.72	1950	1860	840	840
Drywall	0.58	0.17	800	800	840	840
Concrete	1.32	1.32	2250	2250	840	840
Insulation	0.07	0.04	24	16	840	1210

Table 2. Average error and maximum difference between computed and field data along with the value of the corresponding field data at time of maximum difference at various locations for first run

Sensor location	Time lapsed (h)	Mean error (%)	Max. temp. difference (°C)	Corresponding field data (°C)
1T	100–1000	13.1	−5.2	19
	1001–1500	4.1	−6.5	23
	1501–3000	3.1	−5.5	20
1M	100–1000	4.7	−3.1	17
	1001–1500	3.0	−3.5	25
	1501–3000	2.3	−3.6	24
1B	100–1000	8.3	−4.3	23
	1001–1500	4.3	−5.1	26
	1501–3000	3.5	−4.9	33
3T	100–1000	8.4	−5.6	19
	1001–1500	4.0	−5.6	27
	1501–3000	3.2	−5.1	24
3B	100–1000	4.7	−2.4	6.1
	1001–1500	1.6	−3.2	27
	1501–3000	1.4	−3.2	27
4M	100–1000	6.4	−4.5	19
	1001–1500	4.1	−3.2	22
	1501–3000	3.2	−3.1	23

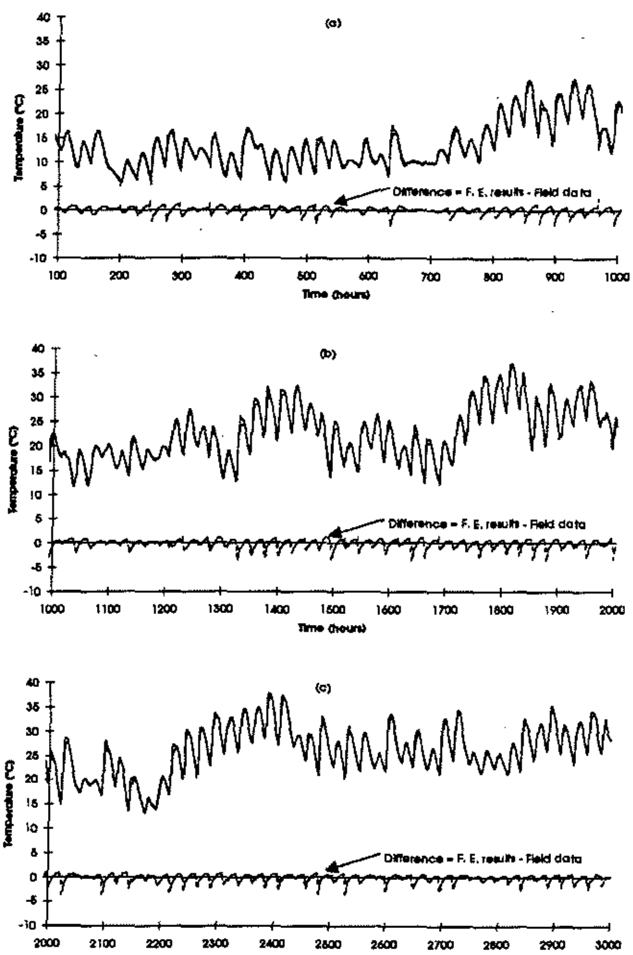

Fig. 9. FE results, field data and the difference between the two values for location 1M; (a) 100–1000 h, (b) 1000–2000 h, (c) 2000–3000 h.

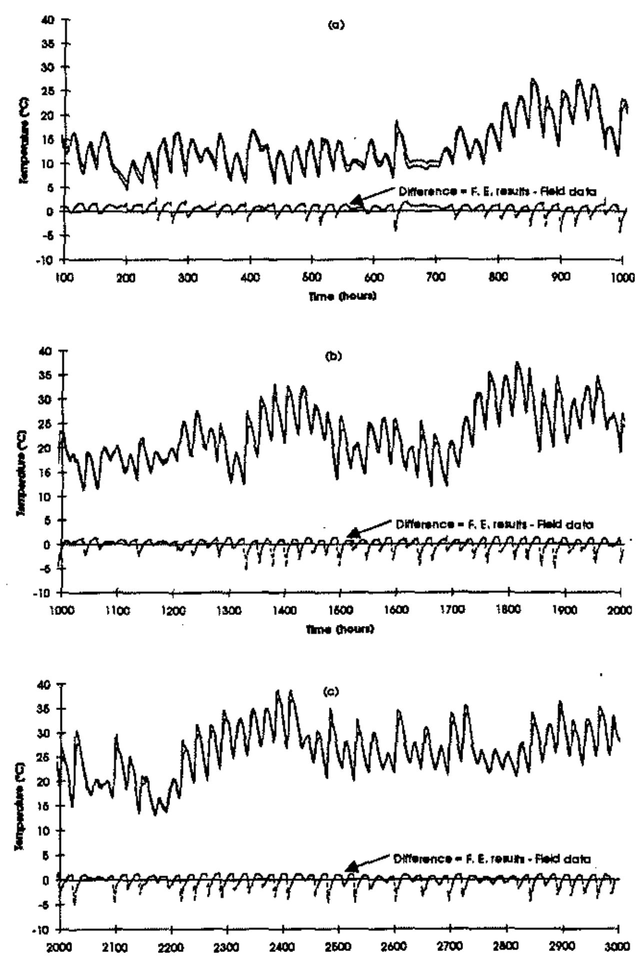

Fig. 10. FE results, field data and the difference between the two values for location 1B; (a) 100–1000 h, (b) 1000–2000 h, (c) 2000–3000 h.

Table 3. Average error and maximum difference between computed and field data along with the value of the corresponding field data at time of maximum difference at various locations for second run

Sensor location	Time lapsed (h)	Mean error (%)	Max. temp. difference (°C)	Corresponding field data (°C)
1T	100–1000	3.9	−6.6	13
	1001–1500	2.5	−7.3	23
1M	100–1000	4.1	−4.2	17
	1001–1500	2.5	−4.4	20
1B	100–1000	3.7	−5.1	18
	1001–1500	2.3	−5.3	26
3T	100–1000	3.9	−6.7	14
	1001–1500	2.5	−5.7	27
3B	100–1500	3.1	−2.3	12
	1001–1500	2.0	−3.7	21
4M	100–1000	5.1	−5.7	19
	1001–1500	2.4	−4.0	22

obtained from the finite element analysis. Figs 8–13 show the analytical and field measured temperatures, and the difference between the two over a period of 3000h (125 days) for location 1T, 1M, 1B, 3T, 3B and 4M. There is a large difference between the initial assumed temperature and the actual value (Figs 8a to 13a). However with time, the results obtained from the FE model do adjust and exhibit the same trend recorded from the field. Furthermore, no numerical oscillation occurs. The curves

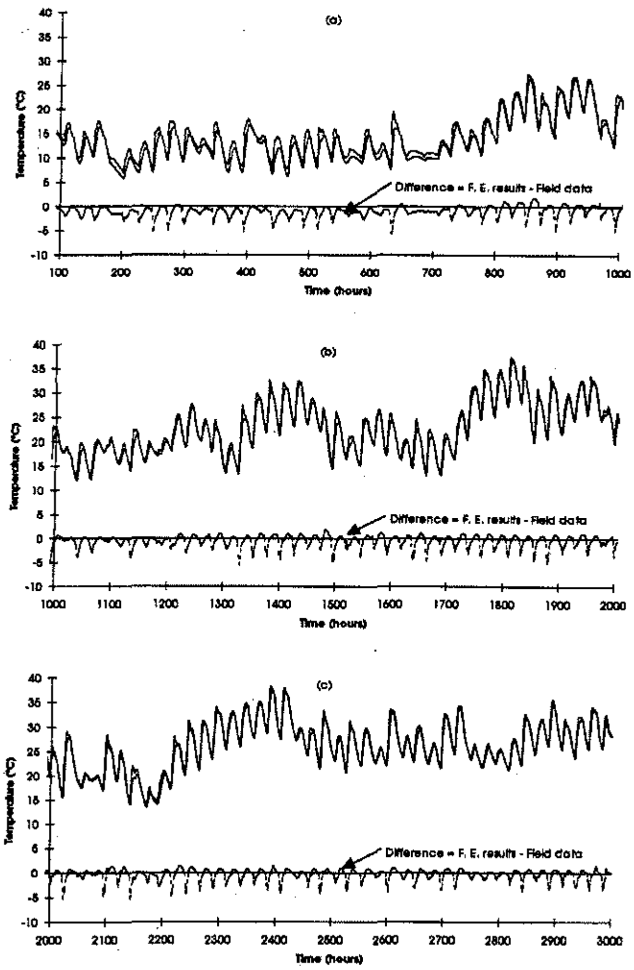

Fig. 11. FE results, field data and the difference between the two values for location 3T; (a) 100–1000 h, (b) 1000–2000 h, (c) 2000–3000 h.

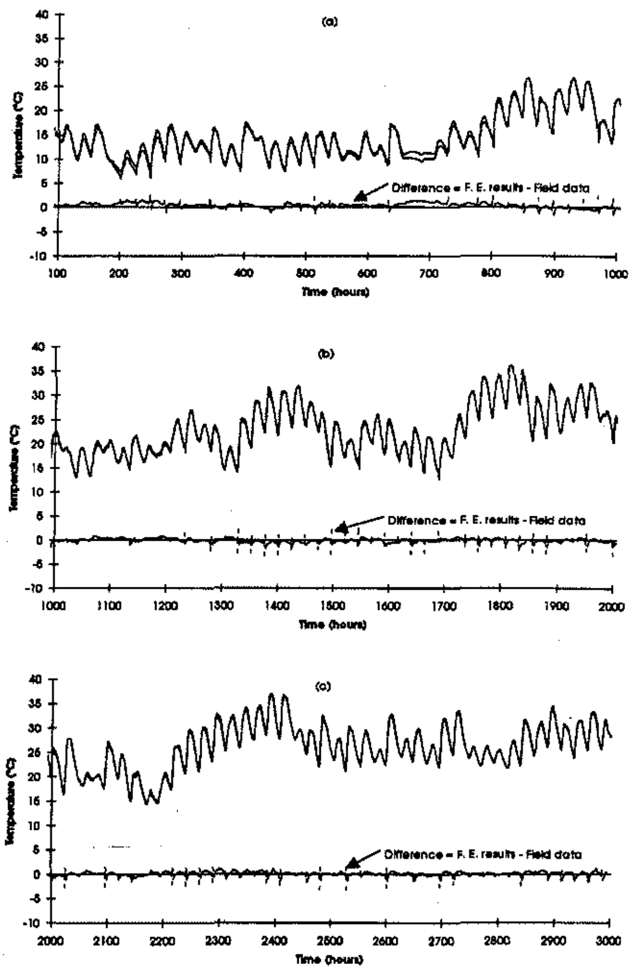

Fig. 12. FE results, field data and the difference between the two values for location 3B; (a) 100–1000 h, (b) 1000–2000 h, (c) 2000–3000 h.

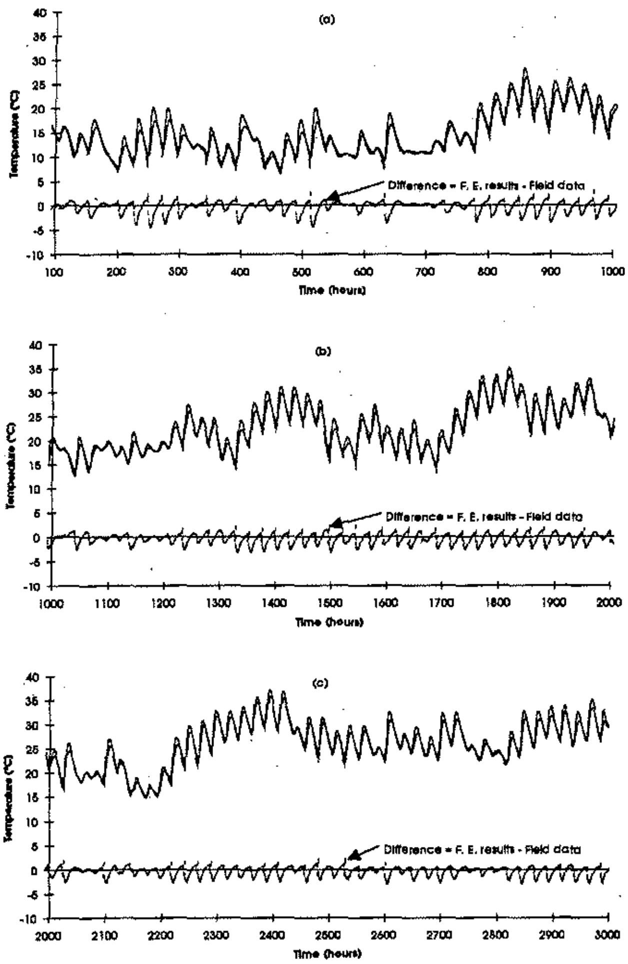

Fig. 13. FE results, field data and the difference between the two values for location 4M; (a) 100–1000 h, (b) 1000–2000 h, (c) 2000–3000 h.

showing the differences between the two values show that the FE results are in good agreement both in terms of phase and size except at daily peaks where the FE data are lower than the experimental value. Table 2 shows the average percentage error and the maximum temperature difference between the computed and recorded data along with the actual value for the recorded data for all six locations. The average errors (percentage differences in hourly readings averaged over the stated time) are all less than 4.3% after the first 1000h. The maximum temperature difference is found to range from 2.4° C to 6.5° C depending on the location of the sensor. The maximum error occurs where there is thermal bridging, ie the sensor is located near the floor level.

A second run is performed using the second set of thermophysical properties in order to investigate the fluctuation in the results caused by using different values reported in the literature. Table 3 summarizes the average percentage error and the maximum temperature difference between the two values along with the field data for 1500h. A maximum difference value of 2.3° C to 7.3° C has been found from the second run in comparison to 2.4° C to 6.5° C from the first run. The maximum error occurs at the same place and the same time for both runs. This implies that although there is a small variation between the two runs, there is little change in the overall thermal behaviour of the wall.

Discussion of results

The discrepancies between the computed and measured data may have several causes; a few are discussed here. Errors associated with the field data are due to measurement uncertainties. These arise mainly from positioning and properly attaching the sensor, ie the actual location of the sensor may vary and/or the bonding between the sensor and the brick may not be perfect. Uncertainties can also be attributed to the accuracy and the calibration of the equipment.

The variations in the finite element results are due to the values used for the thermophysical properties, the boundary conditions, and initial value of the temperature field, and the FE discretization of the wall. A full sensitivity analysis is required to check the effects of the thermophysical properties, but the limited investigation performed here suggests that the overall variations due to changes in the thermophysical properties are small and that acceptable results can be obtained when using values reported in the literature.

As boundary conditions in this study, two measured values are used for the outside wall surfaces and one for the inside surface at approximately mid-height. The computed results indicate that the values of the sensors nearest to the floor level exhibit the largest variations and this is attributed to the presence of the concrete floor slab. The actual outside surface temperature in the vicinity of the concrete slab is different from the mid-height value due to the thermal bridging effect. Here, this phenomenon has been suppressed on the outside surface by imposing a constant boundary condition. Although this is an aproximation in the analysis, one can refine the analysis by monitoring the location where thermal bridging is expected and then insert these values as another boundary condition. The current values are still acceptable provided the focus is on the overall behaviour of the wall.

Like all dynamic analysis, one must assess the effects of initial value used for the temperature field on the overall accuracy of the solution. In this study, an extreme condition was used and it is found that the results obtained from the model converge to the field data rapidly. Moreover, no numerical oscillation was observed during the course of the analysis. This suggests that by using a more representative temperature as the initial value, the variations due to the initial value will become insignificant after a shorter period.

The geometrical representation of the wall is always a source of error since the as-built condition may differ from the building plans. Also the spatial discretization error is always present when representing a wall; research is being done to minimize it using error estimation procedures [9].

One advantage of mathematical modelling is that the temperature at any location inside the wall can be examined. Figure 14 displays the temperature distribution near the concrete floor; the effect of thermal bridging is evident.

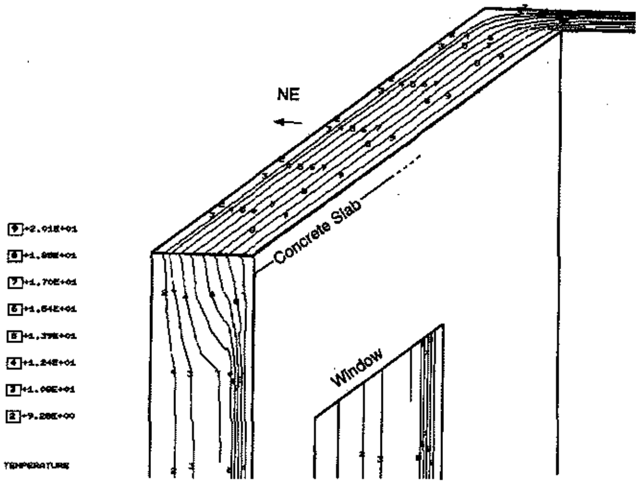

Fig. 14. Temperature distribution around the top corner of the NE wall.

The same procedure can be used to collect and analyse field data to investigate the effects of thermal upgrading. By adjusting the FE model to reflect the proposed new insulation, one can examine if any unfavourable conditions can occur before implementing the upgrade.

Another possibility is the investigation of deterioration such as frost damage. However, to properly investigate freeze-thaw cycles, both the temperature field and the moisture content need to be computed in order to determine the number of freezing cycles that different parts of the masonry wall undergo during a year. This is part of an ongoing research programme.

Thermal deformations and stresses are a function of the thermal regime. Thus, the computed temperature can be used to quantify the thermal strains needed for stress analyses. This type of analysis can be used to investigate the effects of deterioration (cracking, etc.) or to explore the structural consequences of thermal upgrading.

Conclusion

A procedure has been presented using mathematical modelling to extend the range of field data. Monitoring together with modelling can be used to determine the temperature history inside a masonry wall system. The variation between the computed and recorded data is small except at peaks where the maximum differences occur.

The effort required to perform dynamic thermal analysis of masonry walls using the proposed procedure is substantially less than a more elaborate field or model analysis. Furthermore, the results obtained here have a higher degree of certainty than just using a mathematical model and offer a broader temperaturé field than obtained by just monitoring.

The potenital use of such procedure is very broad since the data computed can be used to investigate deterioration problems, to check risks associated with any proposed thermal upgrading, and to perform stress analyses.

References

1. Zienkiewicz, O. C. (1977) *The Finite Element Method*. McGraw-Hill.
2. Chidiac, S. E., Brimacombe, J. K. and Samarasekera, I. V. (1993) A new transient method for the analysis of solidification in the continuous casting of metals, *Applied Scientific*, Netherlands (in press).
3. Hutcheon, N. B. and Handegord, G. O. P. (1989) *Building Science for a Cold Climate*. Construction Technology Center Atlantic Inc., Fredericton.
4. Incropera, F. P. and DeWitt, D. P. (1985) *Introduction to Heat Transfer*. John Wiley & Sons.
5. Maurenbrecher, A. H. P. and Suter, G. T. (1993) Frost damage to clay brick in a load bearing masonry building, *Canadian Journal of Civil Engineering*, **20**, 247–53.
6. Maurenbrecher, A. H. P. and Suter, G. T. (1989) A load bearing clay brick masonry deterioration problem: monitoring of temperature and moisture, in *Proceedings of the 5th Canadian Masonry Symposium*, University of British Columbia, Vancouver, 771–9.
7. Chidiac, S. E. (1993) Finite element refinement for solving transient heat conduction problems, *Int. J. of Numer. Meth. for Heat & Fluid Flow*, submitted.
8. AFEMS (1992) *Finite Element Computer Program, User Manual*. FEM Engineering Corp., Inglewood.
9. Robert, E. J., Hassan, O., Morgan, K. and Peraire, J. (1992) Adaptive explicit and implicit finite element methods for transient thermal analysis, *Int. J. Numer. Methods Engng* **35**, 655–70.